


# DRP1 promotes lactate utilization in *KRAS*-mutant non-small-cell lung cancer cells

Mangze Hu<sup>1</sup> | Yu Zhao<sup>1</sup> | Yuejiao Cao<sup>2</sup> | Qianru Tang<sup>1</sup> | Ziqin Feng<sup>1</sup> | Jun Ni<sup>2,3</sup> | Xiaorong Zhou<sup>1,4</sup> 

<sup>1</sup>Department of Immunology, School of Medicine, Nantong University, Nantong, China

<sup>2</sup>Department of Rehabilitation, The Affiliated Hospital of Nantong University, Nantong, China

<sup>3</sup>Department of Rehabilitation Medicine, The First Affiliated Hospital of Fujian Medical University, Fujian, China

<sup>4</sup>Nantong Key Laboratory of Translational Medicine in Cardiothoracic Diseases, and Research Institution of Translational Medicine in Cardiothoracic Diseases in Affiliated Hospital of Nantong University, Jiangsu, China

## Correspondence

Xiaorong Zhou, Department of Immunology, Nantong University, School of Medicine, 19 Qixiu Road, Nantong, Jiangsu 226001, China.

Email: zhouxiaorong@ntu.edu.cn

Jun Ni, Department of Rehabilitation, The Affiliated Hospital of Nantong University, 20 Xisi Road, Nantong, Jiangsu 226001, China. Email: Nijun@ntu.edu.cn

## Funding information

Jiangsu Six Elite Units Foundation, Grant/Award Number: WSW-058; Jiangsu Key Foundation of Social Development, Grant/Award Number: BE2018670; Nantong Science and technology project, Grant/Award Number: XG202008-5; National Natural Science Foundation of China, Grant/Award Number: 81771681

## Abstract

Metabolic alterations are well documented in various cancers. Non-small-cell lung cancers (NSCLCs) preferentially use lactate as the primary carbon source, but the underlying mechanisms are not well understood. We developed a lactate-dependent cell proliferation assay and found that dynamin-related protein (DRP1), which is highly expressed in *KRAS*-mutant NSCLC, is required for tumor cells to proliferate and uses lactate as fuel, demonstrating the critical role of DRP1 in the metabolic reprogramming of NSCLC. Metabolic and transcriptional profiling suggests that DRP1 orchestrates a supportive metabolic network to promote lactate utilization and redox homeostasis in lung cancer cells. DRP1 suppresses the production of reactive oxygen species (ROS) and protects cells against oxidative damage by enhancing lactate utilization. Moreover, targeting DRP1 not only reduces HSP90 expression but also enhances ROS-induced HSP90 cleavage, thus inhibiting activation of mitogen activated protein kinase and PI3K pathways and leading to suppressed lactate utilization and increased ROS-induced cell death. Taken together, these results suggest that DRP1 is a crucial regulator of lactate metabolism and redox homeostasis in *KRAS*-mutant lung cancer, and that targeting lactate utilization by modulating DRP1 activity might be an effective treatment for lung cancer.

## KEY WORDS

cancer metabolism, DRP1, *KRAS* mutation, lactate, lung cancer

Mangze Hu and Yu Zhao are the co-first authors.

This is an open access article under the terms of the Creative Commons Attribution-NonCommercial License, which permits use, distribution and reproduction in any medium, provided the original work is properly cited and is not used for commercial purposes.

© 2020 The Authors. *Cancer Science* published by John Wiley & Sons Australia, Ltd on behalf of Japanese Cancer Association.

## 1 | INTRODUCTION

Although metabolic alterations are important hallmarks of cancer, tumors of different tissue origins may adopt different metabolic programs.<sup>1</sup> *KRAS* mutations occur in approximately 30% of lung adenocarcinomas and are the primary oncogenic drivers of non-small-cell lung cancer (NSCLC).<sup>2</sup> Many studies have shown that mutant *KRAS* plays a key role in the metabolic reprogramming of cancer cells by orchestrating multiple metabolic pathway alterations.<sup>3,4</sup> It was thought that mitochondria were dysfunctional in cancer cells, resulting in persistently enhanced glucose uptake and glycolysis (the Warburg effect), but recent studies have demonstrated that despite histological and genetic heterogeneity, human lung tumors concurrently oxidize glucose through glycolytic and oxidative phosphorylation (OXPHOS) pathways.<sup>3,5,6</sup> Studies using a mouse model of *KRAS*-mutant lung cancer also demonstrated that mitochondrial metabolism is essential for tumor growth and that disruption of mitochondrial function reduced lung tumorigenesis.<sup>7,8</sup>

Interestingly, human NSCLC tumors actively take up lactate from circulation and use it as the primary source of energy to support tumor growth.<sup>5</sup> Lactate was once considered a waste product of glycolysis, and it was thought that pyruvate is generated in proliferating tumor cells through the glycolysis pathway, which consumes NAD<sup>+</sup>, and then pyruvate is converted to lactate by lactate dehydrogenase (LDH), which is important because LDH simultaneously converts NADH back to NAD<sup>+</sup>, replenishing the cytosolic NAD<sup>+</sup> pool and allowing glycolysis to persist. Moreover, to maintain pH homeostasis inside the cell, the resulting lactate needs to be secreted into circulation.<sup>9</sup> In lung cancer cells, the influx of extracellular lactate, followed by its conversion to pyruvate for OXPHOS in mitochondria, could presumably suppress glycolytic flow. Therefore, it is intriguing that lung tumors can metabolize glucose through both the glycolysis and OXPHOS pathways while actively taking up lactate from circulation. We hypothesize that lung cancer cells have adopted a unique metabolic program that enables them to use lactate as the primary fuel for tumor progression.

Here, we show that dynamin-related protein (DRP1), which is encoded by the *DNM1L* gene, is required for lactate utilization in *KRAS*-mutant lung cancer cells. DRP1 has been reported to be a regulator of mitochondrial dynamics and is responsible for mitochondrial division in many cell types.<sup>10-12</sup> High levels of DRP1 cause apoptosis of nerve cells and neurodegeneration in vitro and in vivo, probably due to increased oxidative damage.<sup>13</sup> DRP1 is also implicated in cancers; for example, DRP1 is highly expressed and required for the progression of a *KRAS*-driven orthotopic pancreatic cancer mouse model.<sup>14</sup> It was also reported that knocking down DRP1 reduced the proliferation of lung cancer cell lines in vitro and suppressed the growth of human lung cancer xenografts.<sup>15</sup> Our findings expand the function of DRP1 and suggest that targeting DRP1-mediated lactate utilization might be a novel therapeutic strategy for the treatment of *KRAS*-mutant lung cancer.

## 2 | MATERIALS AND METHODS

### 2.1 | Cell lines and cell culture

Beas-2B and A549 cells were purchased from FuHeng Biology. H1975 and H358 cells were obtained from Herb Source Biotechnology, and H460 and H23 cells were from ATCC. Beas-2B and A549 cells were cultured in high glucose DMEM, and H1975, H358, H460 and H23 cells were cultured in RPMI-1640 medium supplemented with 10% FBS and 1% penicillin/streptomycin. Cells were grown at 37°C in an incubator in a 5% CO<sub>2</sub> in air atmosphere. The lentiviral vector pLX304-*KRAS*<sup>G12V</sup> was used as previously described to generate cells expressing *KRAS*<sup>G12V</sup>.<sup>16</sup> The LentiCRISPR technique and single-cell cloning were used to generate *DNM1L*-knockout cell lines. Sequences of the single guide RNA (sgRNA) targeting the *DNM1L* gene or control sgRNA are as follows: *DNM1L*, GCCTGTAGGTGATCAACCT and Control, CGCTTCCGCGGCCCGTTCAA.

### 2.2 | Cell proliferation and colony formation assays

Cell proliferation was examined with a CCK8 assay, and the soft agar assay was performed as previously described.<sup>16</sup> For the tumor-sphere formation assay, 500 cells were seeded in 96-well ultra-low attachment plates (Corning Inc) with DMEM supplemented with 2% B-27 supplement (Invitrogen), 10 ng/mL basic fibroblast growth factor (Novus), 20 ng/mL epidermal growth factor (PeproTech), 5 µg/mL insulin (Solarbio), and 0.4% bovine serum albumin (Absin). Colonies were counted after 7 d of incubation.

### 2.3 | Flow cytometry analysis (FACS)

Apoptosis was detected with a PE-Annexin V apoptosis detection kit (BD Pharmingen), and reactive oxygen species (ROS) were measured with the Total ROS Assay Kit 520 nm (Thermo Fisher), according to the manufacturer's instructions, followed by FACS analysis using a flow cytometer (ACEA Bioscience).

### 2.4 | Immunofluorescence and confocal imaging

Cells were fixed to glass coverslips with 4% paraformaldehyde for 20 min and then permeabilized with 0.1% Triton X-100 for 20 min. Immunofluorescence staining was performed using a primary antibody against Tom20 (1:100, Cell Signaling Technology) and secondary anti-mouse IgG labeled with Alexa Fluor 488 (1:100, Cell Signaling Technology). Cells were mounted with ProLong Gold Antifade Mountant with DAPI (Thermo Fisher). Images were captured using a confocal microscope (Leica) and were processed using ImageJ software.

## 2.5 | Measuring superoxide dismutase (SOD) activity, glutathione (GSH) levels, NAD<sup>+</sup>/NADH and NADP/NADPH ratios

SOD activity was measured using the SOD Typed Colorimetric Assay Kit (Elabscience), glutathione was measured using the Glutathione Fluorometric Assay Kit (BioVision), and NAD<sup>+</sup>/NADH and NADP/NADPH ratios were measured using the NAD<sup>+</sup>/NADH Quantification Kit (Sigma) and NADP/NADPH assay kit (Abcam), respectively, according to the manufacturers' instructions.

## 2.6 | Transcriptional and metabolic profiling

RNA-seq was performed by Novogene. Differential expression analysis was performed using the DESeq2 R package (1.16.1), and the genes with adjusted *P*-values < .05 were designated differentially expressed genes (DEGs). Gene Ontology (GO) enrichment analysis was performed using the clusterProfiler R package, in which the gene length bias was corrected. GO terms with corrected *P*-values < .05 were considered significantly enriched. Metabolic profiling with liquid chromatography mass spectrometry (LC-MS) was performed by SENSICHP, and the results were analyzed based on the HMDB (<https://hmdb.ca/>) and METLIN (<https://metlin.scripps.edu/>) datasets.

## 2.7 | Transfection, western blotting and data mining

Materials and methods for siRNA transfection in lung cancer cells, western blotting, and The Cancer Genome Atlas (TCGA) data mining are available in Supplementary Material Doc S1.

## 2.8 | Statistical analysis

Statistical analyses were conducted using GraphPad Prism 7 software (GraphPad Software). In general, values were plotted as the mean ± standard deviation (SD). Comparisons of means between independent groups were conducted using Student *t* test (2 groups) or Kruskal-Wallis one-way ANOVA (3 or more groups) with pairwise comparisons, and a *P*-value < .05 was considered statistically significant. Supplemental materials and methods are available in the Doc S1.

# 3 | RESULTS

## 3.1 | DRP1 is upregulated in KRAS-mutant lung adenocarcinomas (LUADs)

To identify genes that are responsible for KRAS-induced metabolic changes, we searched for genes that were differentially expressed between KRAS-mutant tumors and KRAS-wild-type LUAD tumors in TCGA database, focusing on DEGs whose levels correlated positively

with the expression of mutant KRAS (*P* < .05, FC > 1.5). As a result, *DNM1L* was identified as one of the genes that strongly correlated with mutant KRAS gene expression and LUAD stages (Figures 1A, S1A,B). Previous studies have suggested that DRP1 is overexpressed in lung cancer,<sup>17</sup> but controversy still exists.<sup>18</sup> Interestingly, by exploring TCGA database, we found that KRAS-mutant LUAD exhibited higher levels of DRP1 than KRAS-wild-type LUAD, whereas EGFR-mutant LUAD tumors displayed lower DRP1 levels than EGFR-wild-type tumors (Figure 1B). LUAD tumors that were categorized by *BRAF* or *TP53* mutational status showed comparable DRP1 expression (Figure 1B).

In KRAS-mutant lung cancer, the mutant KRAS genes are frequently amplified and overexpressed and contributed to distinctive metabolic reprogramming that promoted aggressive tumor growth and metastasis.<sup>19</sup> Copy number variation (CNV) analysis also indicated that DRP1 expression in LUAD was correlated positively with KRAS gene amplification (Figure 1C). These results suggested that DRP1 expression may be regulated by mutant KRAS. To test this hypothesis, we treated several lung cancer cell lines with the MEK inhibitor PD-0325901, which blocks the mitogen activated protein kinase (MAPK) pathway cascade (RAS/RAF/MEK/ERK). As expected, PD-0325901 inhibited the expression of both DRP1 and p-DRP1 in A549 (KRAS<sup>G12S</sup>) and H460 (KRAS<sup>Q61H</sup>) cells, this inhibition was consistent with findings in a previous study showing that DRP1 is phosphorylated at Ser-616 by ERK (Figure 1D).<sup>20</sup> In H1975 cells harboring EGFR mutations, PD-0325901 also inhibited DRP1 and p-DRP1 levels, demonstrating the involvement of MAPK signaling in DRP1 regulation in these cells (Figure 1D). The levels of both p-DRP1 and DRP1 in H1299 cells (KRAS<sup>WT</sup>) were not changed significantly by PD-0325901, suggesting that DRP1 might be regulated by a MAPK-independent mechanism in the KRAS wild-type cells (Figure 1D). Treatment with mdivi-1, which is considered a DRP1 inhibitor but may function as a mitochondrial complex I inhibitor,<sup>21</sup> reduced DRP1 phosphorylation at Ser616 but not total DRP1 levels in the KRAS and EGFR-mutant cells.

ARS-1620 is an inhibitor that explicitly targets mutant KRAS<sup>G12C</sup> proteins. In H23 cells (KRAS<sup>G12C</sup>), DRP1 and p-ERK levels were suppressed by ARS-1620 (Figure 1E). H358 cells are very sensitive to ARS-1620 (Figure S1C). Surprisingly, these cells quickly developed drug resistance to ARS-1620, and DRP1 expression was correlated positively with levels of ERK activation, again suggesting a close relationship between DRP1 and mutant KRAS (Figure 1F). To further test whether DRP1 is regulated by mutant KRAS-mediated signaling, we introduced mutant KRAS<sup>G12V</sup> cDNA into Beas-2B cells, which are derived from normal bronchial epithelium. Western blot analysis showed that KRAS<sup>G12V</sup>-expressing Beas-2B (KB) cells exhibited increased levels of both DRP1 and p-ERK (Figure 1G).

## 3.2 | DRP1 is critical for lactate utilization in glutamine-free medium

When cultured in conventional medium containing glutamine, lung cancer cells did not utilize lactate and adding lactate suppressed

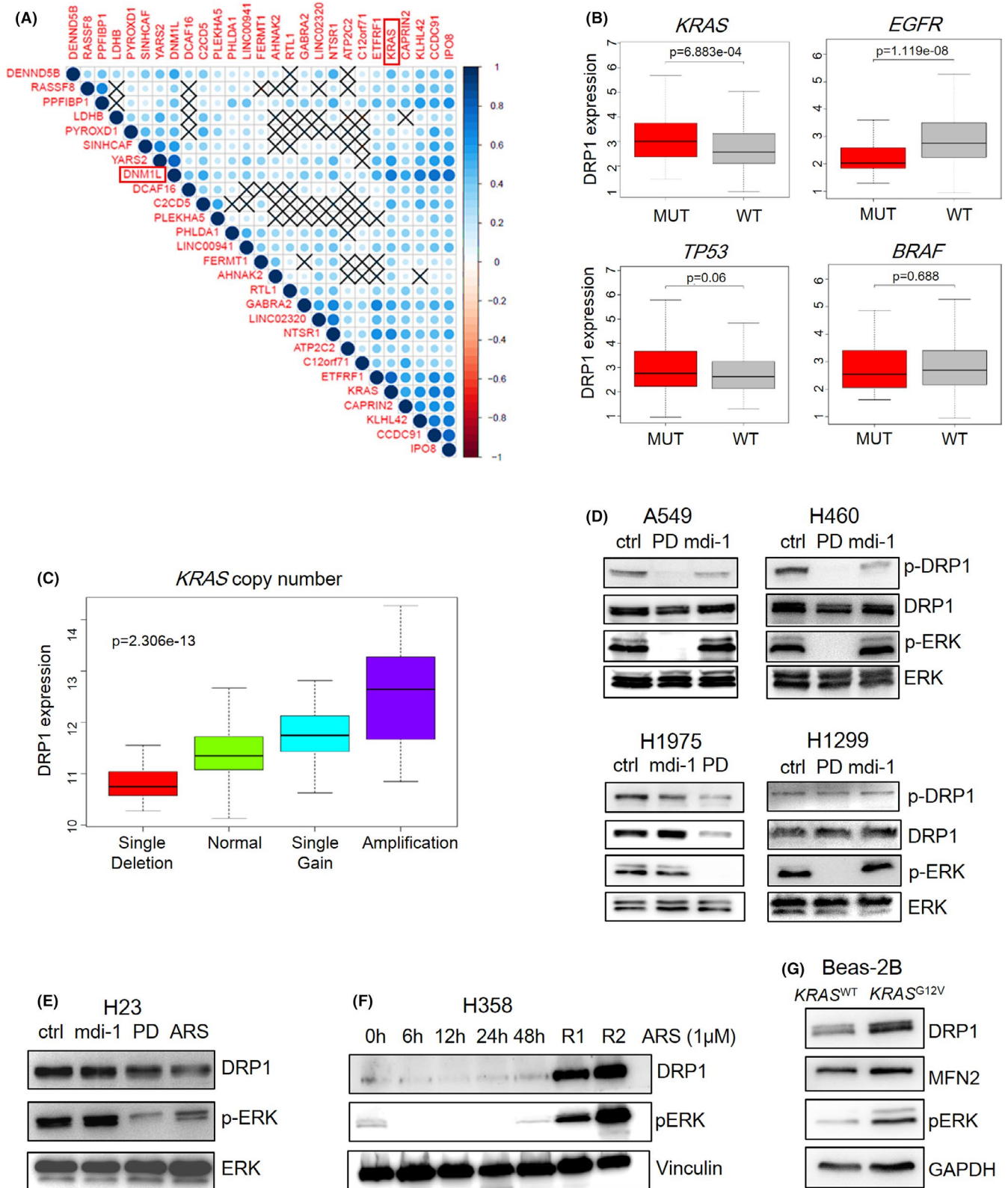


**FIGURE 1** DRP1 is regulated by mutant *KRAS*. A, The genes whose levels were upregulated in *KRAS*-mutant LUAD and correlated with the levels of *KRAS*. B, DRP1 expression in LUAD with or without mutations in *KRAS* or *EGFR*. C, The correlation between DRP1 expression and *KRAS* copy number in LUAD. D, Western blot showing the levels of DRP1, p-DRP1, ERK, and p-ERK in lung cancer cells treated with PD-0325901 (1 μmol/L) or mdivi-1 (50 μmol/L) or mdivi-1 + PD. E, Western blot showing the levels of DRP1, ERK, and p-ERK in H23 cells treated with PD-0325901, mdivi-1, or ARS-1620 (500 nmol/L). F, Western blot showing the levels of DRP1 and p-ERK in H358 cells treated with ARS-1620 for the indicated periods and in drug-resistant H358 cells collected 2 wk (R1) and 6 wk (R2) after treatment. Vinculin was used as a loading control. G, The levels of DRP1, MFN2, and p-ERK in KB cells were determined by western blotting

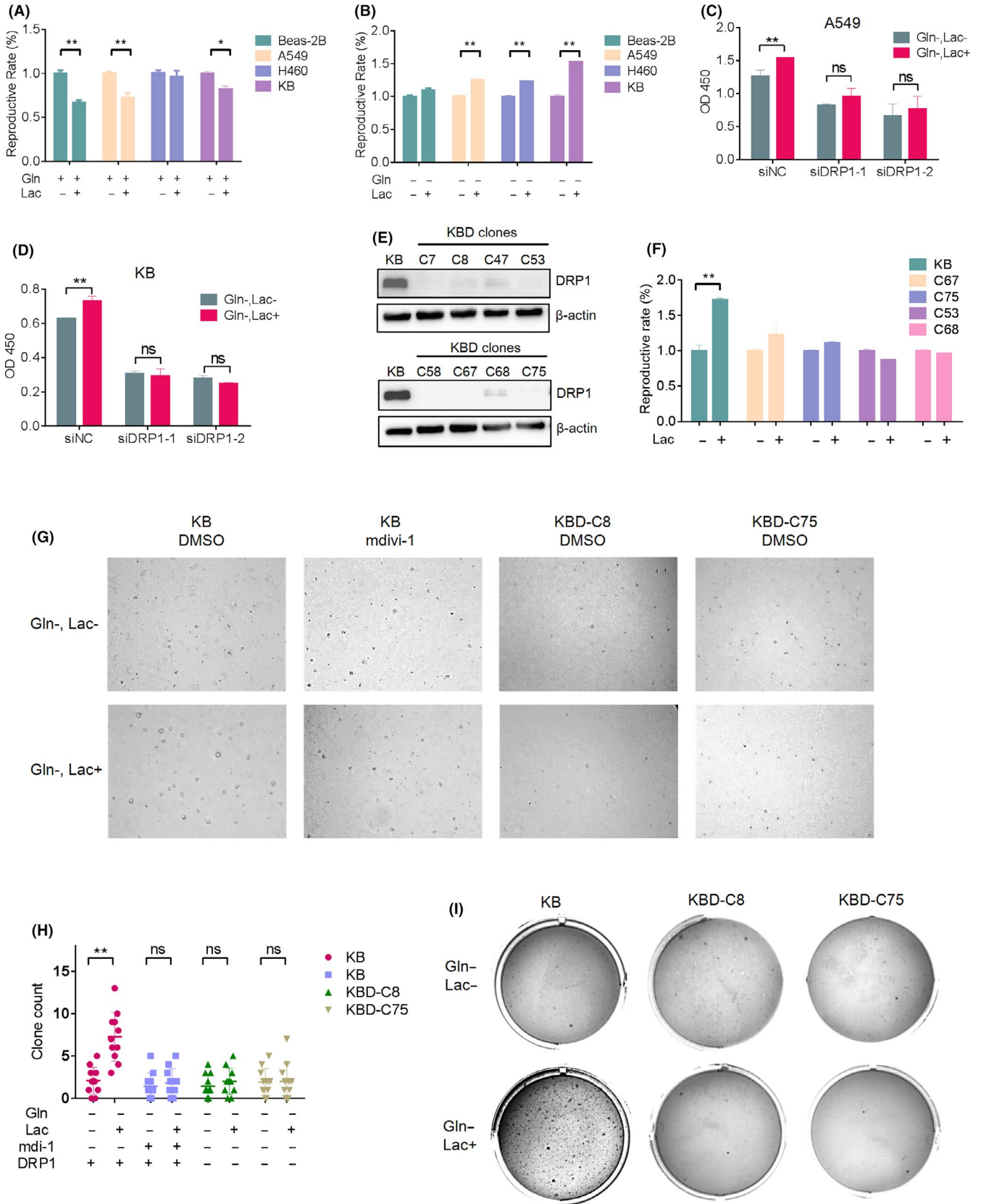


**FIGURE 2** DRP1 promotes the utilization of lactate in Gln<sup>-</sup> medium. A, B, CCK8 assays showing that lactate (Lac) affected cell proliferation with or without glutamine (Gln<sup>+</sup> or Gln<sup>-</sup>). C, D, CCK8 assays showing the effects of DRP1 silencing on cell proliferation. E, The loss of DRP1 in KBD cells was confirmed by western blotting. F, CCK8 assays showing the growth of KB and KBD cells. G, Tumorsphere formation assays demonstrating the anchorage-independent growth of KB and KBD cells. H, Quantification of the results in G. I, Soft agar assay demonstrating the colony formation of KB and KBD cells. The data are shown as the mean  $\pm$  SD ( $n \geq 3$ ). \* $P < .05$ , \*\* $P < .01$

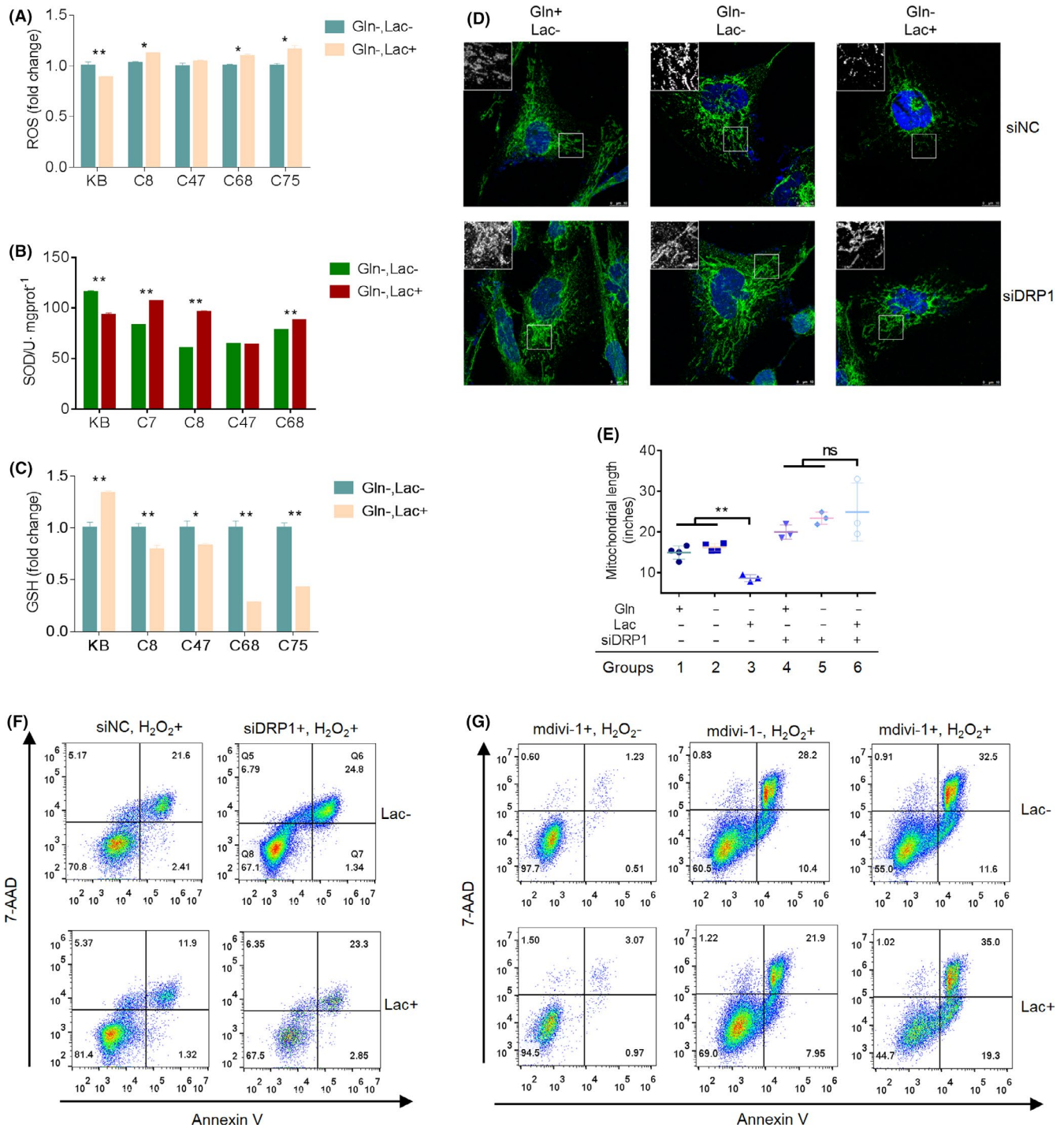


**FIGURE 3** DRP1 regulates metabolic pathways. A-C, The levels of ROS, SOD, and GSH in KB and KBD cells were measured 24 h after adding lactate. D, Confocal imaging showing the mitochondrial network. E, Quantification of the results in E;  $P = .0116$  for group 1 vs group 4;  $P = .0006$  for group 2 vs group 5. F, Apoptosis was induced in control KB cells or DRP1-knockdown KB cells by treatment with H<sub>2</sub>O<sub>2</sub> (0.5 mmol/L) for 2 h, and the percentage of apoptotic cells (Annexin V-positive staining) was determined by FACS analysis. G, The effects of mdivi-1 and lactate on KB cell apoptosis were determined by FACS analysis. All data in bar graphs are the mean  $\pm$  SD ( $n \geq 3$ ). \* $P < .05$ , \*\* $P < .01$

cell proliferation (Figure 2A). Park et al<sup>22</sup> showed that breast cancer cells could metabolize lactate in vitro when glucose was unavailable. However, culture in glucose-free medium caused severe cell death in lung cancer cells, which prevented us from harvesting enough live cells for further studies (Figure S2A,B). Studies suggest that lung

tumors take up very little glutamine from circulation in vivo,<sup>5,8</sup> and glutaminase (GLS), the critical enzyme for glutamine metabolism, is dispensable for tumor growth in a mouse model of lung cancer.<sup>8</sup> Therefore, we removed glutamine and assessed cell growth in the presence or absence of lactate at various concentrations. While

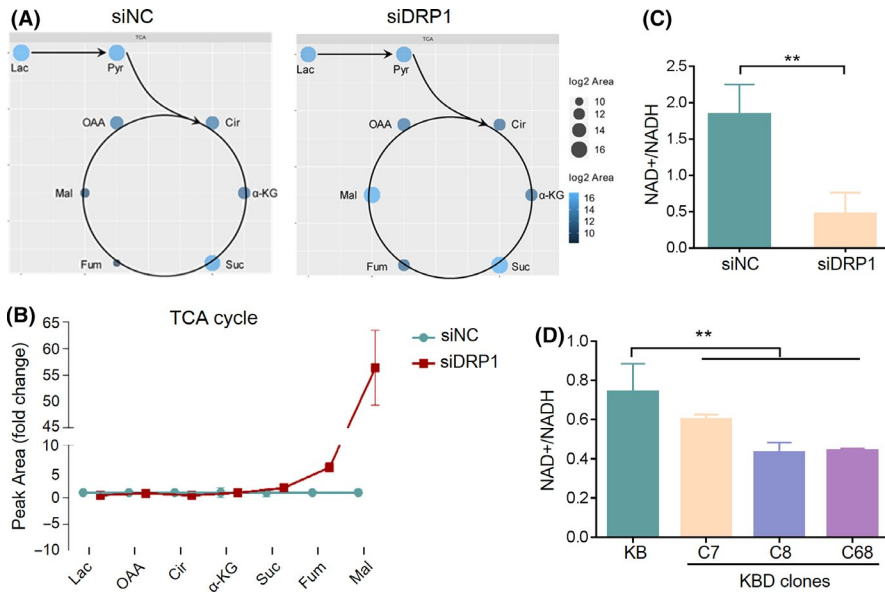


**FIGURE 4** DRP1 regulates redox homeostasis. A, B, TCA cycle intermediates were determined by LC-MS. C, The ratio of NAD<sup>+</sup>/NADH was derived from the LC-MS results. D, The ratio of NAD<sup>+</sup>/NADH in KB and KBD cells was determined by the colorimetric assay. The data are shown as the mean  $\pm$  SD ( $n \geq 3$ ). \* $p < .05$ , \*\* $p < .01$

glutamine deprivation (Gln<sup>-</sup>) suppressed lung cancer cell proliferation by approximately 30%-40%, cell viability was well maintained. Importantly, adding lactate (Lac<sup>+</sup>, 8 mmol/L) significantly enhanced cell proliferation, suggesting that glutamine deprivation altered the metabolic programs in lung cancer cells for lactate utilization (Figure 2B). The proliferation-promoting effect of lactate was more dramatic in KB cells than in Beas-2B cells, suggesting that the effects were associated with *KRAS* mutations (Figure 2B). The amount of lactate used was within a physiological range, as the concentration of lactate in circulation is approximately 1.5-3 mmol/L and can be up to 10-30 mmol/L in cancer tissues.<sup>23</sup> Therefore, we established a condition in which lactate was utilized to promote lung cancer cell proliferation.

Silencing DRP1 diminished the ability of lung cancer cells to use lactate for proliferation (Figure 2C,D and Figure S2C), suggesting that DRP1 is essential for this process. *DNM1L*-knockout cell lines were then established, and the complete loss of DRP1 expression was confirmed by western blotting (Figure 2E). These DRP1-depleted KB (KBD) cells grew normally in conventional medium but grew significantly slower than the control KB cells in Gln<sup>-</sup> and Lac<sup>+</sup> conditions (Figure 2F). Moreover, lactate promoted colony formation of KB cells in the tumorsphere formation assay, but the effects were diminished with KBD cells or in the presence of mdivi-1 (Figure 2G,H). KBD cells also failed to use lactate to promote colony formation in the soft agar assay (Figure 2I). Collectively, these findings suggested that DRP1 is indispensable for lung cancer cells to use lactate for proliferation in glutamine-free conditions.

### 3.3 | Lactate improves redox homeostasis in a DRP1-dependent way

Drp1 depletion in mouse Purkinje cells led to increased oxidative damage and neurodegeneration.<sup>24</sup> We reasoned that active lactate oxidation would increase ROS levels and that DRP1 might be

essential for lung cancer cells to control potential oxidative damage. To test this hypothesis, we measured ROS levels before and 24 h after lactate treatment in Gln<sup>-</sup> conditions. We found that, after adding lactate, ROS levels decreased in KB cells but increased in KBD cells (Figure 3A). As a result, KBD cells displayed higher SOD activity and reduced levels of GSH 24 h after lactate was added (Figure 3B,C). These findings suggested that, instead of causing more oxidative stress, lactate metabolism improves the ability of lung cancer cells to neutralize excessive ROS and, importantly, this effect requires intact DRP1 function.

Silencing DRP1 caused mitochondrial fusion in KB cells, as indicated by the increased mitochondrial lengths in DRP1 knockdown cells (Figure 3D,E), this was consistent with previous studies showing that DRP1 promoted mitochondrial fission.<sup>15,20</sup> Interestingly, lactate induced significant mitochondrial division in KB cells, but this phenomenon was lost in DRP1-knockdown KB cells (Figure 3E). Therefore, lactate utilization not only requires intact DRP1 but also enhances DRP1-mediated mitochondrial division.

To further test the effects of lactate on ROS balance, we treated the cells with H<sub>2</sub>O<sub>2</sub> (0.5 mmol/L) for 2 h. FACS analysis demonstrated that lactate suppressed apoptosis in control KB cells, but the protective effects largely disappeared upon DRP1 knockdown (Figure 3F). Lactate also suppressed H<sub>2</sub>O<sub>2</sub>-induced apoptosis in KB cells treated with DMSO, but not in cells treated with mdivi-1 (Figure 3G). Collectively, these findings suggested that lactate metabolism protects cells against endogenous and exogenous ROS in a DRP1-dependent way.

### 3.4 | DRP1 regulates multiple metabolic pathways

Metabolic profiling was conducted to study how DRP1 regulates lactate metabolism. Interestingly, DRP1 knockdown did not significantly alter the levels of lactate and pyruvate in KB cells or most intermediates of the tricarboxylic acid (TCA) cycle, except that the

levels of malate and fumarate were significantly increased upon DRP1 knockdown (Figure 4A,B). We found that the NAD<sup>+</sup>/NADH ratio was reduced in DRP1-knockdown cells (Figure 4C,D). As NADH is mainly generated in mitochondria through the TCA cycle, these findings suggested that DRP1 depletion may not significantly impair mitochondrial OXPHOS in KB cells. Further analysis revealed that both the glycolysis and Warburg effect pathways were marginally enhanced upon DRP1 knockdown, but did not reach statistical significance (Figure S3A). Nevertheless, these findings suggested that DRP1 may make lung cancer cells less reliant on glycolysis for energy supply when lactate is available. The levels of some significant metabolites and their related pathways are shown in Figure S3B.

### 3.5 | DRP1 promotes a lactate supportive metabolic network

Metabolic profiling indicated that the GSH/GSSG and NADPH/NADP<sup>+</sup> ratios decreased in DRP1-knockdown cells, and this was confirmed using 2 DRP1-knockdown cell lines (Figure 5A,B). As NADPH is required for the conversion of GSSG to GSH for redox homeostasis,<sup>25</sup> we reasoned that the decreased GSH/GSSG ratio in DRP1-depleted cells was probably due to a shortage in NADPH supply. The malic enzyme 1 (ME1)-dependent NADPH supply is critical for redox balance in various cancers.<sup>26,27</sup> We found that ME1 levels were reduced in DRP1-depleted cells (Figure 5C-E),

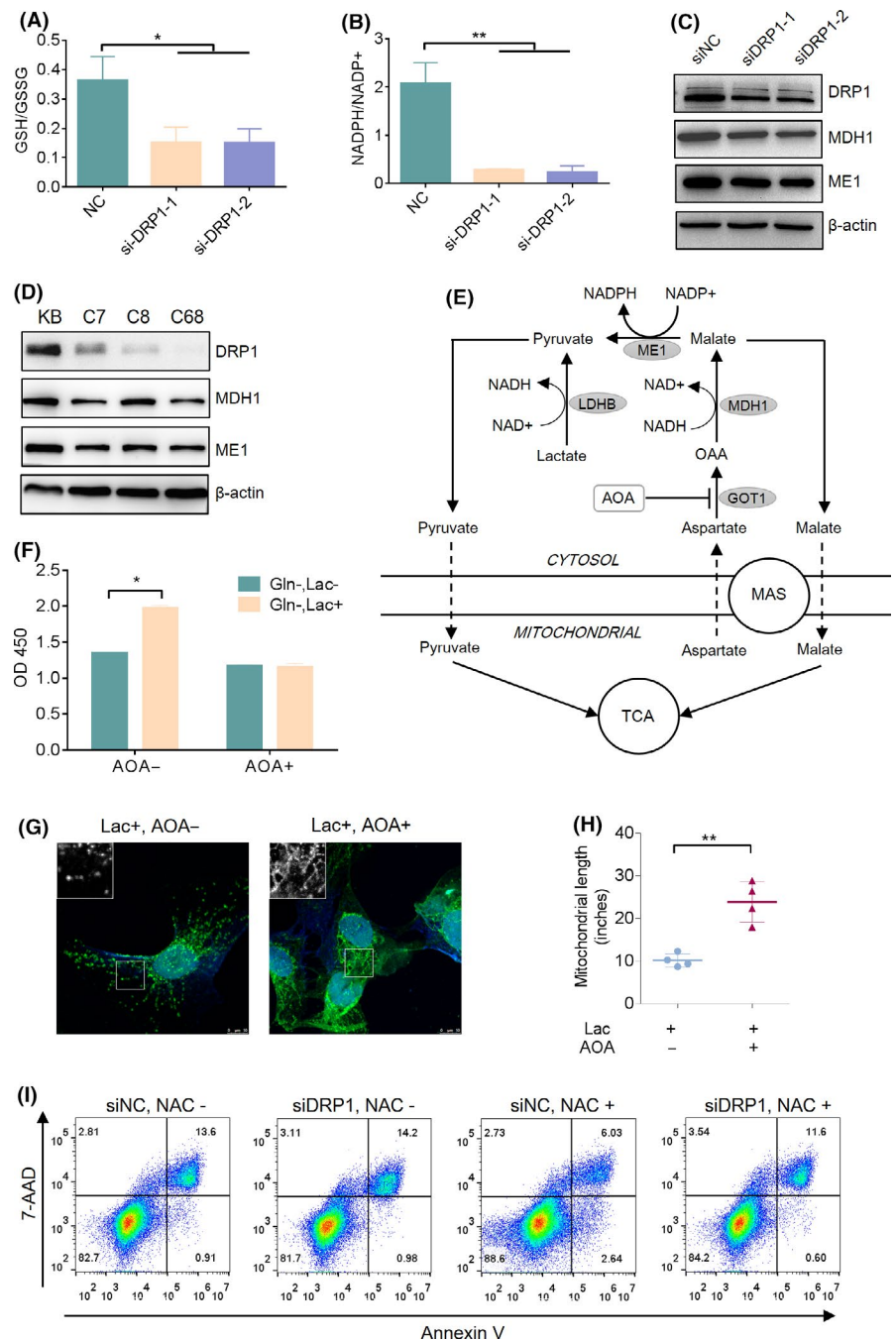


**FIGURE 5** DRP1 regulates a lactate supportive metabolic network. A, B, The ratio of GSH/GSSG and NADPH/NADP<sup>+</sup> in control or DRP1-knockdown KB cells. C, D, Western blot showing the levels of MDH1 and ME1 in KB or KBD cells. E, Diagram showing the lactate metabolism-supportive network. F, KB cells were pretreated with 1.0 mmol/L AOA for 24 h, and lactate-induced cell proliferation was determined by CCK8 assays. G, Mitochondrial elongation was determined with confocal imaging. H, Quantification of the results in H. I, The effects of 5 mmol/L NAC treatment for 24 h on H<sub>2</sub>O<sub>2</sub>-induced apoptosis were determined by FACS analysis. In all experiments, KB cells were cultured under Gln<sup>-</sup> conditions, and the data are shown as the mean ± SD (n ≥ 3). \*P < .05, \*\*P < .01



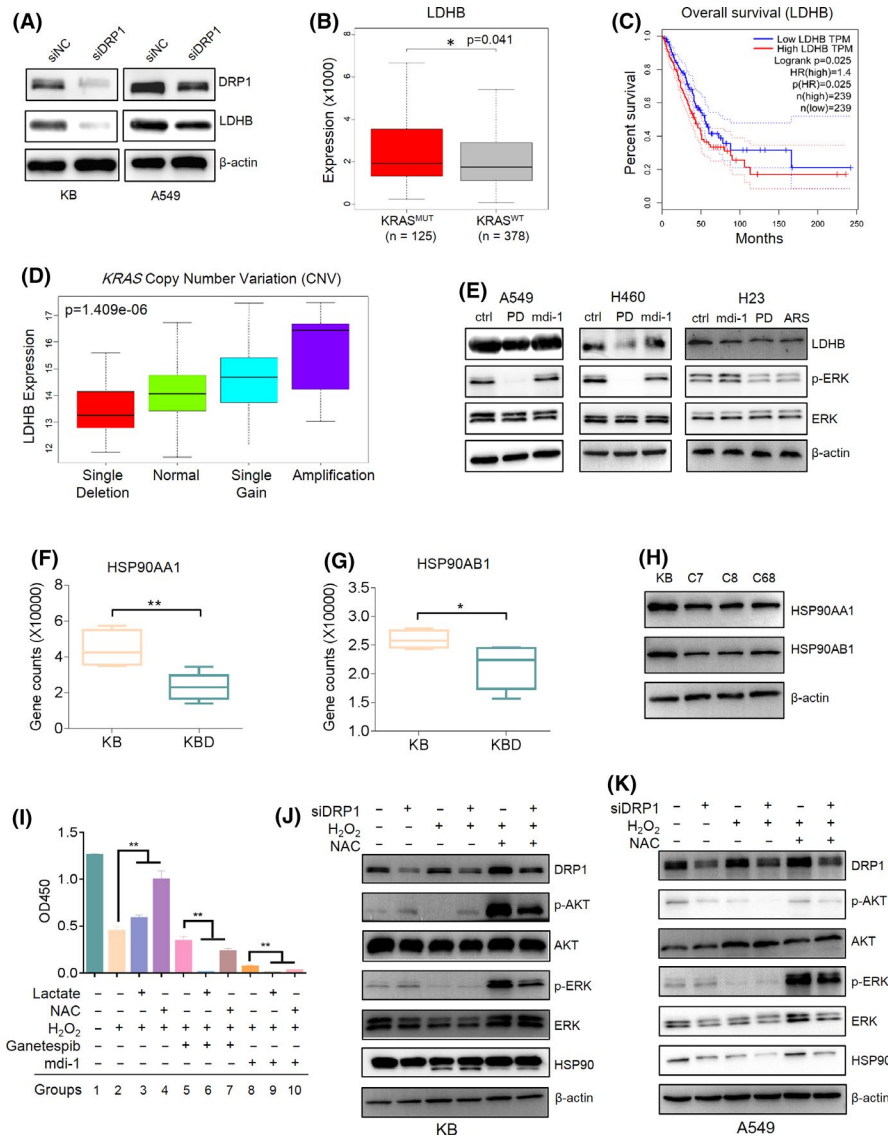


**FIGURE 6** DRP1-regulated genes and pathways. A, Western blot analysis of LDHB levels in KB and A549 cells. B, The levels of LDHB in KRAS-mutant or wild-type LUAD tumors. C, Overall survival of LUAD patients grouped by LDHB expression levels. D, Positive correlation between LDHB and the copy number of the KRAS gene. E, Western blot analysis showing the levels of LDHB, p-ERK, and ERK in lung cancer cells with the indicated treatment. The HSP90AA1 and HSP90AB1 levels in KB and KBD cells were obtained from the results of RNA-seq (F, G) and measured by western blot (H). I, KB cells were treated with ganetespiib (500 nmol/L), mdi-1 (50  $\mu$ mol/L), NAC (1 mmol/L), lactate (8 mmol/L), or H<sub>2</sub>O<sub>2</sub> (10  $\mu$ mol/L) alone or in combination as indicated in the graph. After 3 d, cell proliferation was evaluated with CCK8 assays. \* $P < .05$  compared with the control. J, K, HSP90 cleavage was induced by H<sub>2</sub>O<sub>2</sub> (0.5 mmol/L) for 2 h, and western blot analysis showed the levels of DRP1, HSP90, ERK, p-ERK, AKT, and p-AKT in KB and A549 cells with treatments as indicated in the graph

suggesting that the decreased NADPH/NADP<sup>+</sup> ratio may be associated with reduced ME1 levels in DRP1-depleted cells. In addition, cytosolic malate dehydrogenase 1 (MDH1) is critical for redox balance by converting NADH to NAD<sup>+</sup> (Figure 5E).<sup>28</sup> The levels of MDH1 were reduced in DRP1 knockdown cells (Figure 5C), this is consistent with the decreased NAD<sup>+</sup>/NADH ratios in DRP1-depleted cells (Figure 3C). These findings suggested that there might be a supportive metabolic network for lactate utilization, as shown in Figure 5E, through which DRP1 promotes lactate utilization in KRAS-mutant lung cancer cells. To test whether the malate-aspartate shuttle (MAS) is involved in lactate utilization, we treated KB cells with AOA, an inhibitor of aspartate aminotransferase, to block the MAS and the metabolic network (Figure 5E). The results indicated that AOA treatment suppressed lactate-induced proliferation in KB cells (Figure 5F). We showed that lactate induced mitochondrial fission only when DRP1 was intact (Figure 3D), however this phenomenon disappeared when MAS was blocked by AOA (Figure 5G,H).

Treatment with the antioxidant *N*-acetyl-L-cysteine (NAC) suppressed ROS-induced apoptosis in KB cells. However, when DRP1 was inhibited, the protective effects of NAC were decreased (Figure 5I). NAC is a precursor of GSH, and recycling GSSG to regenerate GSH required NADPH.<sup>29</sup> Because of NADPH deficiency, it is not surprising that NAC could not adequately protect DRP1 knockdown cells from ROS-induced apoptosis. Collectively, these results suggested that DRP1 regulates a metabolic network to maintain redox balance when lactate is metabolized.

### 3.6 | Transcriptional profiling revealed DRP1-regulated genes and pathways

Transcriptional profiling identified multiple DRP1-regulated genes and pathways (Figure S4A,B). Notably, lactate metabolism was significantly suppressed upon DRP1 knockdown (Figure S4B). By analyzing the DEGs, we found that lactate dehydrogenase B (LDHB)

expression was downregulated in KBD cells compared with that in KB cells. lactate dehydrogenase A (LDHA) preferentially converted lactate to pyruvate, whereas LDHB favored the reverse reaction.<sup>9</sup> Western blot analysis confirmed that DRP1 inhibition reduced LDHB expression in lung cancer cells (Figure 6A). TCGA analysis showed that LDHB was highly expressed in *KRAS*-mutant LUAD and associated with *KRAS* copy numbers and survival times (Figure 6B-D). Treatment with PD-032590 reduced the levels of LDHB in lung cancer cell lines (Figure 6E). However, treatment with mdivi-1 did not consistently inhibit LDHB in the tested cell lines (Figure 6E).

Downregulation of HSP90 upon DRP1 depletion caught our attention (Figure 6F-H). HSP90 supports a large number of client proteins that are implicated in various cancer-related signaling pathways.<sup>30</sup> In addition, ROS induce HSP90 cleavage and apoptosis.<sup>31</sup> We found that in KB cells cultured without glutamine, adding lactate or NAC could reduce cell death induced by 10  $\mu\text{mol/L}$   $\text{H}_2\text{O}_2$  treatment for 3 d (Figure 6I, groups 1-4), but these effects were inhibited by the HSP90 inhibitor ganetespib, and adding lactate actually caused more cell death in the presence of ganetespib (Figure 6I, groups 5-7). In addition, pretreatment with mdivi-1 greatly sensitized the cells to  $\text{H}_2\text{O}_2$ -induced cell death, and the protective effects of lactate or NAC were also diminished by mdivi-1 (Figure 6I, groups 8-10).

DRP1 knockdown suppressed the levels of HSP90, confirming the RNA-seq results (Figure 6J). We showed that 0.5 mmol/L  $\text{H}_2\text{O}_2$  treatment for 2 h quickly induced HSP90 cleavage (Figure 6J).  $\text{H}_2\text{O}_2$  treatment also reduced the levels of p-AKT and p-ERK, suggesting that excessive ROS and the resulting HSP90 cleavage dampen oncogenic pathways (Figure 6J). Treatment with NAC alleviated HSP90 cleavage; as a result, the levels of HSP90 were increased (Figure 6J). Importantly, these effects seemed to depend on DRP1 because, in DRP knockdown cells, the NAC-mediated recovery of HSP90 was diminished (Figure 6J). Surprisingly, treatment with  $\text{H}_2\text{O}_2$  + NAC markedly induced p-AKT and p-ERK (Figure 6J), suggesting that intermediate ROS could enhance the oncogenic pathway, which is consistent with a recent study showing that NAC accelerated a mouse model of *KRAS*-mutant lung cancer.<sup>32</sup> However, in DRP-depleted cells, the induction of p-AKT and p-ERK by  $\text{H}_2\text{O}_2$  + NAC was greatly diminished (Figure 6J). We obtained similar results with A549 cells

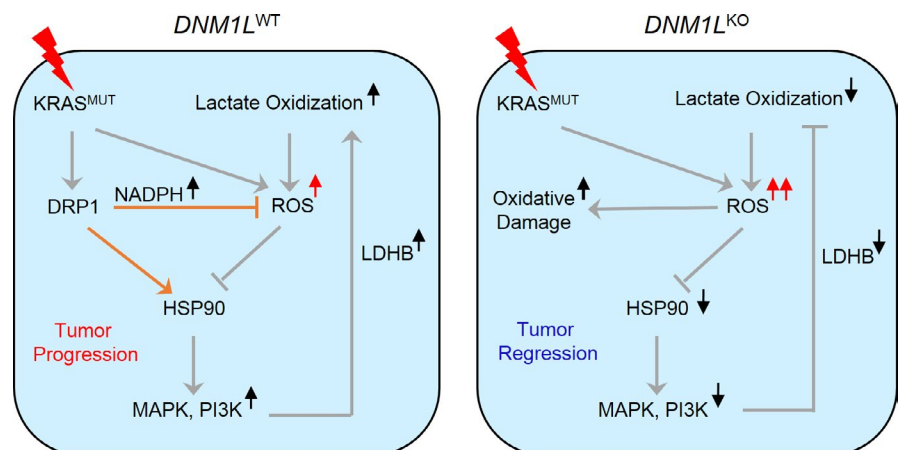
(Figure 6K). These findings suggested that DRP1 regulates HSP90 at both the transcriptional and posttranscriptional levels and thus modulate the activation of oncogenic pathways.

## 4 | DISCUSSION

Lactate, once considered a dead-end product of glycolysis, is emerging as an essential regulator of multiple biological processes, including tumor metabolism, the immune response, and signal transduction.<sup>23,33</sup> Increased lactate uptake is a characteristic of lung cancer metabolism.<sup>5</sup> Here, we showed that *KRAS*-mutant lung cancer cells use lactate to not only provide energy but also prevent ROS-induced oxidative damage, thereby promoting cell proliferation. Importantly, DRP1, previously known as a key regulator of mitochondrial dynamics,<sup>11</sup> plays a critical role in lactate utilization in lung cancer cells.

*KRAS* mutation has been linked to high oxidative stress in lung cancer cells,<sup>34,35</sup> and when lactate is actively oxidized, excessive ROS are generated in mitochondria; if not neutralized, excessive ROS may cause oxidative damage and hinder tumor growth. In addition, the conversion of lactate to pyruvate by LDH would likely interfere with  $\text{NAD}^+$  recycling. Our results suggest that the upregulated DRP1 in *KRAS*-mutant lung cancer is able to resolve these conflicts, as depicted in our model (Figure 7). However, when DRP1 is inhibited, redox control is impaired, lactate utilization is suppressed and, consequently, lung cancer cells may become more reliant on glycolysis and susceptible to ROS-induced apoptosis. This model is in agreement with the findings from a patient with the *DNM1L* gene mutation.<sup>36</sup> The patients showed abnormal development of the nervous system and persistently elevated lactate levels in the blood and died at the age of 37 d.<sup>36</sup> The elevated lactate was thought to be caused by enhanced glycolysis and lactate production due to suppressed mitochondrial respiration.<sup>36</sup> However, the roles of DRP1 in mitochondrial division and respiration seem to vary depending on cell type and physiological context. For example, skin fibroblasts isolated from the abovementioned patient showed normal respiratory capacity, and analysis of muscle biopsy samples from the patient

**FIGURE 7** The model of DRP1-dependent lactate utilization. DRP1 is highly expressed in *KRAS*-mutant lung cancer cells and promotes lactate oxidation and ROS neutralization. DRP1 enhanced HSP90 function and thus augmented the activation of MAPK and PI3K pathways, leading to tumor progression. In contrast, DRP1 inhibition disrupted cellular homeostasis in *KRAS*-mutant cancer cells and eventually leads to tumor regression



did not reveal defects in mitochondrial networking.<sup>36</sup> Recently, Dai et al showed that DRP1 depletion did not affect oxidative metabolism in lung cancer cell lines cultured in conventional medium. However, when Drp1 was deleted in mouse Purkinje cells, which highly express Drp1, mitochondrial respiration was decreased, and Purkinje cells underwent apoptosis due to oxidative damage.<sup>13</sup> Based on these findings, as well as our findings, we hypothesized that suppressed lactate utilization contributed to the elevated blood lactate levels in the patient and that the loss of the DRP1-mediated redox balance might be the underlying mechanism of the developmental defects in the patient's nervous system, as neurons are highly sensitive to oxidative damage.<sup>37</sup>

Targeting DRP1 suppresses the growth of lung cancer cells in vitro and in vivo.<sup>38</sup> Recently, in a KRAS-driven mouse model of pancreatic cancer, mice with pancreatic tissue-specific Drp1 knockout exhibited prolonged survival compared with that of their wild-type counterparts, although the tumor burden was similar between the 2 groups, suggesting that targeting DRP1 may benefit pancreatic cancer treatment.<sup>14</sup> Our study suggested that DRP1 might be a promising therapeutic target, especially in KRAS-driven lung cancer. Notably, Drp1 knockout caused embryonic lethality in mice, suggesting the requirement of Drp1 for normal development,<sup>39</sup> and the patient with the DRP1 mutation had a devastating outcome.<sup>36</sup> Therefore, targeting DRP1 has to be carefully monitored, as it might result in unwanted side effects. We found that HSP90 is involved in the function of DRP1 in KRAS-mutant lung cancer cells, although the precise mechanism needs further investigation. The antitumor effects of HSP90 inhibitors in lung cancer models, as single agents or in combination with other drugs, have been demonstrated, and novel HSP90 inhibitors are under development.<sup>40-42</sup> We suggest that targeting lactate utilization by modulating DRP1, or more practically by inhibiting HSP90, might be useful for the treatment of KRAS-mutant lung cancer.

## ACKNOWLEDGMENTS

This work was supported by the National Natural Science Foundation of China (Grant number 81771681 to XZ), the Jiangsu Key Foundation of Social Development (Grant number BE2018670 to JN), the Jiangsu Six Elite Units Foundation (Grant number WSW-058 to XZ), and the Nantong Science and technology project (Grant number XG202008-5 to XZ).

## DISCLOSURE

The authors have no conflicts of interest to declare.

## ORCID

Xiaorong Zhou  <https://orcid.org/0000-0002-6120-7318>

## REFERENCES

- DeBerardinis RJ, Chandel NS. Fundamentals of cancer metabolism. *Sci Adv*. 2016;2:e1600200.
- Ferrer I, Zugazagoitia J, Herberth S, John W, Paz-Ares L, Schmid-Bindert G. KRAS-Mutant non-small cell lung cancer: from biology to therapy. *Lung Cancer*. 2018;124:53-64.
- Kerr EM, Martins CP. Metabolic rewiring in mutant Kras lung cancer. *FEBS J*. 2018;285:28-41.
- Kawada K, Toda K, Sakai Y. Targeting metabolic reprogramming in KRAS-driven cancers. *Int J Clin Oncol*. 2017;22:651-659.
- Faubert B, Li KY, Cai L, et al. Lactate metabolism in human lung tumors. *Cell*. 2017;171(2):358-371 e359.
- Hensley C, Faubert B, Yuan Q, et al. Metabolic heterogeneity in human lung tumors. *Cell*. 2016;164:681-694.
- Weinberg F, Hamanaka R, Wheaton WW, et al. Mitochondrial metabolism and ROS generation are essential for Kras-mediated tumorigenicity. *Proc Natl Acad Sci USA*. 2010;107:8788-8793.
- Davidson S, Papagiannakopoulos T, Olenchock B, et al. Environment impacts the metabolic dependencies of Ras-driven non-small cell lung cancer. *Cell Metab*. 2016;23:517-528.
- Urbanska K, Orzechowski A. Unappreciated role of LDHA and LDHB to control apoptosis and autophagy in tumor cells. *Int J Mol Sci*. 2019;20:2085.
- van der Blik AM, Shen Q, Kawajiri S. Mechanisms of mitochondrial fission and fusion. *Cold Spring Harb Perspect Biol*. 2013;5:a011072.
- Fonseca TB, Sanchez-Guerrero A, Milosevic I, Raimundo N. Mitochondrial fission requires DRP1 but not dynamins. *Nature*. 2019;570:E34-E42.
- Buhlman L, Damiano M, Bertolin G, et al. Functional interplay between Parkin and Drp1 in mitochondrial fission and clearance. *Biochim Biophys Acta*. 2014;1843:2012-2026.
- Kageyama Y, Zhang Z, Roda R, et al. Mitochondrial division ensures the survival of postmitotic neurons by suppressing oxidative damage. *J Cell Biol*. 2012;197:535-551.
- Nagdas S, Kashatus JA, Nascimento A, et al. Drp1 promotes KRAS-driven metabolic changes to drive pancreatic tumor growth. *Cell Rep*. 2019;28(7):1845-1859 e1845.
- Rehman J, Zhang HJ, Toth PT, et al. Inhibition of mitochondrial fission prevents cell cycle progression in lung cancer. *FASEB J*. 2012;26:2175-2186.
- Zhou X, Updegraff BL, Guo Y, et al. PROTOCADHERIN 7 Acts through SET and PP2A to potentiate MAPK signaling by EGFR and KRAS during lung tumorigenesis. *Cancer Res*. 2017;77:187-197.
- Chiang Y-Y, Chen S-L, Hsiao Y-T, et al. Nuclear expression of dynamin-related protein 1 in lung adenocarcinomas. *Mod Pathol*. 2009;22:1139-1150.
- Kim YY, Yun SH, Yun J. Downregulation of Drp1, a fission regulator, is associated with human lung and colon cancers. *Acta Biochim Biophys Sin*. 2018;50:209-215.
- Kerr EM, Gaude E, Turrell FK, Frezza C, Martins CP. Mutant Kras copy number defines metabolic reprogramming and therapeutic susceptibilities. *Nature*. 2016;531:110-113.
- Kashatus J, Nascimento A, Myers L, et al. Erk2 phosphorylation of Drp1 promotes mitochondrial fission and MAPK-driven tumor growth. *Mol Cell*. 2015;57:537-551.
- Bordt EA, Clerc P, Roelofs BA, et al. The putative Drp1 inhibitor mdivi-1 is a reversible mitochondrial complex I inhibitor that modulates reactive oxygen species. *Dev Cell*. 2017;40(6):583-594 e586.
- Park S, Chang CY, Safi R, et al. ERRalpha-regulated lactate metabolism contributes to resistance to targeted therapies in breast cancer. *Cell Rep*. 2016;15:323-335.
- de la Cruz-Lopez KG, Castro-Munoz LJ, Reyes-Hernandez DO, Garcia-Carranca A, Manzo-Merino J. Lactate in the regulation of tumor microenvironment and therapeutic approaches. *Front Oncol*. 2019;9:1143.
- Yamada T, Adachi Y, Fukaya M, Iijima M, Sesaki H. Dynamin-related protein 1 deficiency leads to receptor-interacting protein kinase 3-mediated necroptotic neurodegeneration. *Am J Pathol*. 2016;186:2798-2802.
- Tong L, Chuang CC, Wu S, Zuo L. Reactive oxygen species in redox cancer therapy. *Cancer Lett*. 2015;367:18-25.

26. Lu Y-X, Ju H-Q, Liu Z-X, et al. ME1 regulates NADPH homeostasis to promote gastric cancer growth and metastasis. *Cancer Res.* 2018;78:1972-1985.
27. Zhu Y, Gu LI, Lin XI, et al. Dynamic regulation of ME1 phosphorylation and acetylation affects lipid metabolism and colorectal tumorigenesis. *Mol Cell.* 2020;77(1):138-149 e135.
28. Gaude E, Schmidt C, Gammage PA, et al. NADH shuttling couples cytosolic reductive carboxylation of glutamine with glycolysis in cells with mitochondrial dysfunction. *Mol Cell.* 2018;69(4):581-593 e587.
29. Arakawa M, Ito Y. N-acetylcysteine and neurodegenerative diseases: basic and clinical pharmacology. *Cerebellum.* 2007;6:308-314.
30. Jego G, Hazoume A, Seigneuric R, Garrido C. Targeting heat shock proteins in cancer. *Cancer Lett.* 2013;332:275-285.
31. Beck R, Dejeans N, Glorieux C, et al. Hsp90 is cleaved by reactive oxygen species at a highly conserved N-terminal amino acid motif. *PLoS One.* 2012;7:e40795.
32. Sayin VI, Ibrahim MX, Larsson E, Nilsson JA, Lindahl P, Bergo MO. Antioxidants accelerate lung cancer progression in mice. *Sci Transl Med.* 2014;6(221):221ra15.
33. Baltazar F, Afonso J, Costa M, Granja S. Lactate beyond a waste metabolite: metabolic affairs and signaling in malignancy. *Front Oncol.* 2020;10:231.
34. Liou G-Y, Döppler H, DelGiorno K, et al. Mutant KRas-induced mitochondrial oxidative stress in acinar cells upregulates EGFR signaling to drive formation of pancreatic precancerous lesions. *Cell Rep.* 2016;14:2325-2336.
35. Hong B-J, Park W-Y, Kim H-R, et al. Oncogenic KRAS sensitizes lung adenocarcinoma to GSK-J4-induced metabolic and oxidative stress. *Cancer Res.* 2019;79:5849-5859.
36. Waterham HR, Koster J, van Roermund CW, Mooyer PA, Wanders RJ, Leonard JV. A lethal defect of mitochondrial and peroxisomal fission. *N Engl J Med.* 2007;356:1736-1741.
37. Wang X, Michaelis EK. Selective neuronal vulnerability to oxidative stress in the brain. *Front Aging Neurosci.* 2010;2:12.
38. Guo X, Disatnik MH, Monbureau M, Shamloo M, Mochly-Rosen D, Qi X. Inhibition of mitochondrial fragmentation diminishes Huntington's disease-associated neurodegeneration. *J Clin Invest.* 2013;123:5371-5388.
39. Wakabayashi J, Zhang Z, Wakabayashi N, et al. The dynamin-related GTPase Drp1 is required for embryonic and brain development in mice. *J Cell Biol.* 2009;186:805-816.
40. Wang L, Fan Y, Mei H, et al. Novel Hsp90 inhibitor C086 potently inhibits non-small cell lung cancer cells as a single agent or in combination with gefitinib. *Cancer Manag Res.* 2019;11:8937-8945.
41. Park K-S, Oh B, Lee M-H, et al. The HSP90 inhibitor, NVP-AUY922, sensitizes KRAS-mutant non-small cell lung cancer with intrinsic resistance to MEK inhibitor, trametinib. *Cancer Lett.* 2016;372:75-81.
42. Acquaviva J, Smith DL, Sang J, et al. Targeting KRAS-mutant non-small cell lung cancer with the Hsp90 inhibitor ganetespib. *Mol Cancer Ther.* 2012;11:2633-2643.

#### SUPPORTING INFORMATION

Additional supporting information may be found online in the Supporting Information section.

**How to cite this article:** Hu M, Zhao Y, Cao Y, et al. DRP1 promotes lactate utilization in KRAS-mutant non-small-cell lung cancer cells. *Cancer Sci.* 2020;111:3588-3599. <https://doi.org/10.1111/cas.14603>